



# Search for time-dependent $CP$ violation in $D^0 \rightarrow \pi^+ \pi^- \pi^0$ decays

LHCb collaboration<sup>†</sup>

## Abstract

A measurement of time-dependent  $CP$  violation in  $D^0 \rightarrow \pi^+ \pi^- \pi^0$  decays using a  $pp$  collision data sample collected by the LHCb experiment in 2012 and from 2015 to 2018, corresponding to an integrated luminosity of  $7.7 \text{ fb}^{-1}$ , is presented. The initial flavour of each  $D^0$  candidate is determined from the charge of the pion produced in the  $D^*(2010)^+ \rightarrow D^0 \pi^+$  decay. The decay  $D^0 \rightarrow K^- \pi^+ \pi^0$  is used as a control channel to validate the measurement procedure. The gradient of the time-dependent  $CP$  asymmetry,  $\Delta Y$ , in  $D^0 \rightarrow \pi^+ \pi^- \pi^0$  decays is measured to be

$$\Delta Y = (-1.3 \pm 6.3 \pm 2.4) \times 10^{-4},$$

where the first uncertainty is statistical and the second is systematic, which is compatible with  $CP$  conservation.

Submitted to Phys. Rev. Lett.

© 2024 CERN for the benefit of the LHCb collaboration. CC BY 4.0 licence.

<sup>†</sup>Authors are listed at the end of this Letter.



Charge-parity ( $CP$ ) symmetry violation in the Standard Model (SM) of particle physics is insufficient to explain the observed baryon asymmetry in the visible universe [1–3]. This suggests the existence of  $CP$ -violating mechanisms beyond the SM, and thus studies of  $CP$  violation are a promising sector to probe for new physics. While  $CP$  violation is experimentally well-established in the mesonic systems containing  $b$  or  $s$  quarks [4–9], direct  $CP$  violation in the decay of charmed hadrons has only recently been observed in the difference between  $D^0 \rightarrow K^+K^-$  and  $D^0 \rightarrow \pi^+\pi^-$  decays [10], and is yet to be conclusively observed in a single decay mode [11]. This Letter presents the first measurement of time-dependent  $CP$  violation in the singly Cabibbo-suppressed decay  $D^0 \rightarrow \pi^+\pi^-\pi^0$ .<sup>1</sup>

In the  $D^0$  meson system, the flavour eigenstates differ from the mass eigenstates. A neutral meson initially in a state of definite flavour can thus evolve in time into its antiparticle, and vice versa. The mass eigenstates are typically written in terms of the flavour eigenstates as  $|D_{1(2)}\rangle = p|D^0\rangle \mp q|\bar{D}^0\rangle$ , where  $p$  and  $q$  are complex numbers. The phase convention  $CP|D^0\rangle = -|\bar{D}^0\rangle$  is adopted with  $CP|D_1\rangle = |D_1\rangle$  in the limit of  $CP$  conservation [12]. The dimensionless parameters  $x \equiv (m_1 - m_2)/\Gamma$  and  $y \equiv (\Gamma_1 - \Gamma_2)/2\Gamma$ ,<sup>2</sup> where  $m_{1(2)}$  and  $\Gamma_{1(2)}$  are the mass and width of the  $|D_{1(2)}\rangle$  mass eigenstate and  $\Gamma = (\Gamma_1 + \Gamma_2)/2$  is the mean width, define the mixing properties. Defining  $A_f$  ( $\bar{A}_f$ ) as the amplitude of the decay  $D^0 \rightarrow f$  ( $\bar{D}^0 \rightarrow f$ ), direct  $CP$  violation occurs if  $|A_f/\bar{A}_f| \neq 1$  for a self-conjugate final state  $f$ . Time-dependent  $CP$  violation occurs in mixing if  $|q/p| \neq 1$ , and in the interference of mixing and decay when  $\phi_f \neq 0$ , where  $\phi_f = \arg(-q\bar{A}_f/pA_f)$ . Since the mixing parameters  $x$  and  $y$  are both  $< 1\%$  in the charm system and  $CP$ -violation effects are small [12, 13], the time-dependent asymmetry for a  $D^0$  meson decaying to a  $CP$  eigenstate,  $f_{CP}$ , can be expanded to first order in the  $D^0$  decay time,  $t$ , as

$$A_{CP}(f_{CP}, t) \equiv \frac{\Gamma_{D^0 \rightarrow f_{CP}}(t) - \Gamma_{\bar{D}^0 \rightarrow f_{CP}}(t)}{\Gamma_{D^0 \rightarrow f_{CP}}(t) + \Gamma_{\bar{D}^0 \rightarrow f_{CP}}(t)} \quad (1)$$

$$\approx a_{f_{CP}}^{\text{dir}} + \Delta Y_{f_{CP}} \frac{t}{\tau_{D^0}}.$$

The constant term  $a_{f_{CP}}^{\text{dir}}$  arises from direct  $CP$  violation,  $\tau_{D^0} = 410.3 \pm 1.0$  fs [14, 15] is the  $D^0$  meson lifetime, and  $\Gamma_{D^0 \rightarrow f_{CP}}(t)$  ( $\Gamma_{\bar{D}^0 \rightarrow f_{CP}}(t)$ ) is the time-dependent decay rate of a  $D^0$  ( $\bar{D}^0$ ) meson to the final state  $f_{CP}$ . Neglecting direct  $CP$  violation, the size of the gradient  $\Delta Y_{f_{CP}}$  becomes independent of the final state and can be approximately expressed in terms of the underlying mixing and  $CP$  violation parameters as [16]

$$\Delta Y_{f_{CP}} \approx \frac{\eta_{f_{CP}}}{2} \left[ \left( \left| \frac{q}{p} \right| + \left| \frac{p}{q} \right| \right) x \sin \phi - \left( \left| \frac{q}{p} \right| - \left| \frac{p}{q} \right| \right) y \cos \phi \right], \quad (2)$$

where  $\eta_{f_{CP}}$  is the  $CP$  eigenvalue of the final state and  $\phi = \arg(q/p)$ . Thus, the gradient can be defined in terms of the universal  $CP$ -violating parameter  $\Delta Y \equiv \eta_{f_{CP}} \Delta Y_{f_{CP}}$ .

The parameter  $\Delta Y$  has been measured in the two-body decay modes  $D^0 \rightarrow \pi^+\pi^-$  and  $D^0 \rightarrow K^-K^+$  by the BaBar [17], CDF [18], Belle [19] and LHCb [20–23] collaborations. Assuming universality of  $\Delta Y$  across all decay modes, the current world average is  $\Delta Y = (0.9 \pm 1.1) \times 10^{-4}$  [12]. The LHCb collaboration has also measured the parameter  $\Delta y = -\Delta Y$  [16] in  $D^0 \rightarrow K_S^0\pi^+\pi^-$  decays [24, 25].

<sup>1</sup>Charge-conjugate decays are implied here and throughout this Letter.

<sup>2</sup>Natural units with  $\hbar = c = 1$  are used throughout.

Phase-space integrated analyses of multi-body  $D^0$  decays have diluted sensitivity to  $\Delta Y$  due to a mixture of  $CP$ -even and  $CP$ -odd contributions from intermediate states [26]. The effective gradient of the time-dependent asymmetry is given by [27]

$$\Delta Y_f^{\text{eff}} = (2F_+^f - 1)\Delta Y, \quad (3)$$

where  $F_+^f$  is the  $CP$ -even fraction of the decay  $D^0 \rightarrow f$ . For the decay  $D^0 \rightarrow \pi^+\pi^-\pi^0$ , the  $CP$ -even fraction has been measured using CLEO- $c$  data to be  $F_+^{\pi\pi\pi} = 0.973 \pm 0.017$  [26], providing almost undiluted sensitivity.

The Cabibbo-favoured decay  $D^0 \rightarrow K^-\pi^+\pi^0$  is used to validate the analysis procedure. Since the decay  $\bar{D}^0 \rightarrow K^-\pi^+\pi^0$  is doubly Cabibbo-suppressed, the final state  $K^-\pi^+\pi^0$  is almost flavour specific. Therefore,  $CP$ -violation effects in mixing and in the interference of mixing and decay are suppressed with respect to the signal channel. The corresponding  $CP$ -violating parameter in this mode,  $\Delta Y_{K\pi\pi}$ , has been estimated from the most recent world averages of the relevant parameters [12–14] to be  $|\Delta Y_{K\pi\pi}| < 2.5 \times 10^{-5}$  at 90% confidence level.

Samples of  $D^0 \rightarrow \pi^+\pi^-\pi^0$  decays are reconstructed from proton-proton ( $pp$ ) collisions collected by the LHCb experiment in 2012 and from 2015 to 2018, corresponding to an integrated luminosity of  $7.7 \text{ fb}^{-1}$  at centre-of-mass energies of  $\sqrt{s} = 8$  and 13 TeV, respectively. Throughout this Letter, the data sample collected in 2012 (2015–18) will be referred to as the Run 1 (2) sample. The flavour of the  $D^0$  meson at production is inferred from the charge of the pion produced in the preceding  $D^*(2010)^+ \rightarrow D^0\pi^+$  decay. The  $D^*(2010)^+$  meson and the pion originating from its decay will be referred to as the  $D^{*+}$  meson and tag pion throughout this Letter, respectively.

The LHCb detector [28, 29] is a single-arm forward spectrometer covering the pseudorapidity range  $2 < \eta < 5$ , designed for the study of particles containing  $b$  or  $c$  quarks. The detector elements that are particularly relevant to this analysis are: a silicon-strip vertex detector surrounding the  $pp$  interaction region that allows a precise measurement of the flight distance of  $D^0$  mesons; a tracking system that provides a measurement of the momentum of the charged particles; a set of ring-imaging Cherenkov detectors that provide charged particle identification; and a calorimeter system which identifies photons and provides a measurement of their energy. The flight distance of the  $D^0$  meson is defined as the distance between its measured decay vertex and the primary  $pp$  interaction vertex (PV). Neutral pions are reconstructed in their diphoton decay. If the energy clusters produced by the two photons in the calorimeter overlap, the candidate is labelled as *merged*; otherwise, the candidate is labelled as *resolved*.

Online event selection is performed by a trigger consisting of a hardware stage, using information from the calorimeter and muon systems, followed by two software stages. In this analysis, no explicit requirements are imposed at the hardware level, since all hardware selections are found to contribute to the sample [30]. At the first software stage in the Run 1 running period, at least one of the charged pions from the  $D^0$  meson decay must satisfy criteria on its momentum,  $\chi_{\text{IP}}^2$  and track quality. The quantity  $\chi_{\text{IP}}^2$  is defined as the difference in the vertex-fit  $\chi^2$  of a PV reconstructed with and without the given track or particle under consideration. For the Run 2 sample either one of the pions from the  $D^0$  decay must satisfy a similar set of criteria, or both of the tracks must satisfy a set of looser criteria and their combined vertex must satisfy additional vertex-quality requirements. At the second software stage, a full or partial reconstruction of the  $D^{*+}$  decay is performed. In the full reconstruction, pairs of oppositely-charged pion candidates

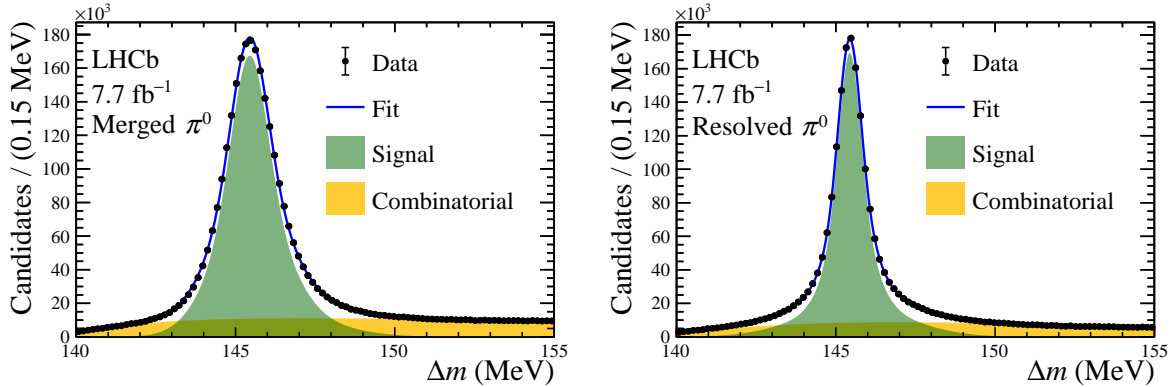


Figure 1: Distributions of  $\Delta m$  in the signal channel after all selection requirements for the (left) merged and (right) resolved  $\pi^0$  categories. The fit used to evaluate the signal yields is also shown.

that form a good-quality vertex are combined. A neutral pion candidate is added to form a  $D^0$  candidate. Finally, the  $D^0$  candidate is combined with a low-momentum charged pion candidate to reconstruct a  $D^{*+}$  candidate. In the partial reconstruction, the  $\pi^0$  candidate is not considered in the trigger. Additional selection criteria are imposed based on momenta, track and vertex quality, and displacement from the PV. For the Run 1 sample, only partially reconstructed candidates are considered with a cut-based selection. For the Run 2 sample, fully reconstructed candidates must satisfy a cut-based selection, while partially reconstructed candidates must fulfil a requirement on the output of a bonsai-Boosted Decision Tree (BDT) classifier [31].

Offline, additional requirements are imposed on kinematic and particle-identification observables. The kinematics of each decay chain are fitted [32] with the constraints that the  $D^{*+}$  meson must originate from a PV and the  $\pi^0$  candidate has its known mass [14]. Secondary decays — where the  $D^{*+}$  meson is produced in the decay of a  $b$  hadron rather than in the initial  $pp$  collision — are suppressed by imposing tight requirements on the flight distance of the  $D^{*+}$  meson and the  $\chi_{\text{IP}}^2$  of the  $D^0$  meson. The mass of the pair of charged pions from the  $D^0$  decay is required to be inconsistent with the known  $K_S^0$  mass [14] to suppress the background from  $D^0 \rightarrow K_S^0 \pi^0$  decays. The background from  $D^0 \rightarrow K^- \pi^+ \pi^0$  decays, where the  $K^-$  meson is misidentified as a pion, is suppressed by requiring  $D^0$  candidates to have a reconstructed mass,  $m(D^0)$ , close to the known value,  $m_{\text{PDG}}(D^0)$  [14]. Candidates in the resolved category must satisfy  $|m(D^0) - m_{\text{PDG}}(D^0)| < 60$  MeV and candidates in the merged sample must satisfy  $-60 < m(D^0) - m_{\text{PDG}}(D^0) < 120$  MeV. Other potential sources of misidentified and misreconstructed backgrounds are found to be negligible. The same requirements are applied to candidates in the control channel, with the exceptions of the particle-identification requirements and the  $K_S^0$  meson veto. The combinatorial background is further suppressed by a set of BDT classifiers trained on the data samples, separately for the merged and resolved  $\pi^0$  categories and for the Run 1 and Run 2 samples. Over-training effects are controlled by training the classifiers on only around 25% (6%) of the data in the Run 1 (2) sample for each  $\pi^0$  reconstruction category, and monitoring the classifiers' performances on equivalently sized testing samples. The same BDT classifiers are applied to the signal and control channels, with different requirements on the output. The selections on the BDT classifier outputs are optimised

by maximising the metric  $N/\sigma_N$ , where  $N$  is the number of signal decays and  $\sigma_N$  is its uncertainty obtained from a fit to the distribution of the  $D^{*+}$  and  $D^0$  mass difference,  $\Delta m \equiv m(D^{*+}) - m(D^0)$ . Finally, when more than one candidate originates from a single event in the final sample, only one is randomly selected. Figure 1 shows the distributions of  $\Delta m$  for all selected candidates in the signal channel, separately for the two  $\pi^0$  reconstruction categories. A sum of three Gaussian distributions is used to model the signal shape. The combinatorial background is modelled by the empirical `ROODSTD0BG` function from the `ROOFIT` software package [33, 34]. Signal yields of 2.3 (18) and 1.5 (20) million are obtained in the signal (control) channel for the merged and resolved categories, respectively.

The data are analysed in subsamples split by data-taking year, magnet polarity and  $\pi^0$  reconstruction category. In order to avoid experimenter’s bias, the results of the analysis were not examined until the full procedure was finalised.

Each data sample is divided into 21 — approximately evenly populated —  $D^0$  decay-time bins in the range  $[0.6, 8.0] \tau_{D^0}$ . The decay time of each  $D^0$  candidate is calculated as the product of the known  $D^0$  mass and its measured flight distance, divided by its measured momentum. The asymmetry in each bin is determined from a binned maximum-likelihood fit to the  $\Delta m$  distributions of selected  $D^0$  and  $\bar{D}^0$  candidates. Determining the yields by fitting the  $\Delta m$  distribution — rather than the  $m(D^0)$  distribution — removes background from real  $D^0$  candidates combined with an erroneously tagged pion. The fits are performed simultaneously to  $D^0$  and  $\bar{D}^0$  candidates, with shared shape parameters but separate yields for the signal and background components. The measured asymmetry is defined as

$$A_{\text{meas}}(\langle t/\tau_{D^0} \rangle_i) \equiv \frac{N_{D^0}^i - N_{\bar{D}^0}^i}{N_{D^0}^i + N_{\bar{D}^0}^i}, \quad (4)$$

where  $N_{D^0}^i$  and  $N_{\bar{D}^0}^i$  are the signal yields of  $D^0$  and  $\bar{D}^0$  decays in a given decay-time bin,  $i$ , respectively. The mean decay time in each bin,  $\langle t/\tau_{D^0} \rangle_i$ , is calculated as a weighted average of the decay time of all candidates in that bin. The weights are defined as the product of a background-subtraction weight and a kinematic correction weight which will be defined in the following paragraph. The gradient of the time-dependent asymmetry is determined from a linear least-squares fit to the measured asymmetries.

The raw asymmetries — defined as the unweighted asymmetries between  $D^0$  and  $\bar{D}^0$  yields — present in each data sample do not correspond to the  $CP$  asymmetry in Equation 1. Rather, they include the production asymmetry of  $D^{*+}$  mesons and some unknown nuisance asymmetries induced by the reconstruction and selection procedure. In particular, the LHCb magnet deflects oppositely-charged tag pions in opposite directions, which induces some kinematic-dependent asymmetries, since the detector is not perfectly symmetrical. Periodically reversing the magnetic field polarity throughout the data-taking only approximately cancels the effect. Such kinematic asymmetries can introduce a time-dependent asymmetry in the presence of correlations between kinematic variables and the decay time of each  $D^0$  candidate induced by the selection criteria. A per-event weighting procedure is applied to correct for the most severe kinematic-dependent asymmetries. Events are weighted, in several stages, to equalise the binned distributions of the curvature and projection angles of the tag-pion track [23], the pseudorapidity of the tag pion and  $D^0$  candidates, and the transverse momentum of the  $D^0$  candidate. Figure 2 shows the measured gradient of the time-dependent asymmetry in each data subsample before and after the kinematic weighting. No significant shift is observed in the signal channel.

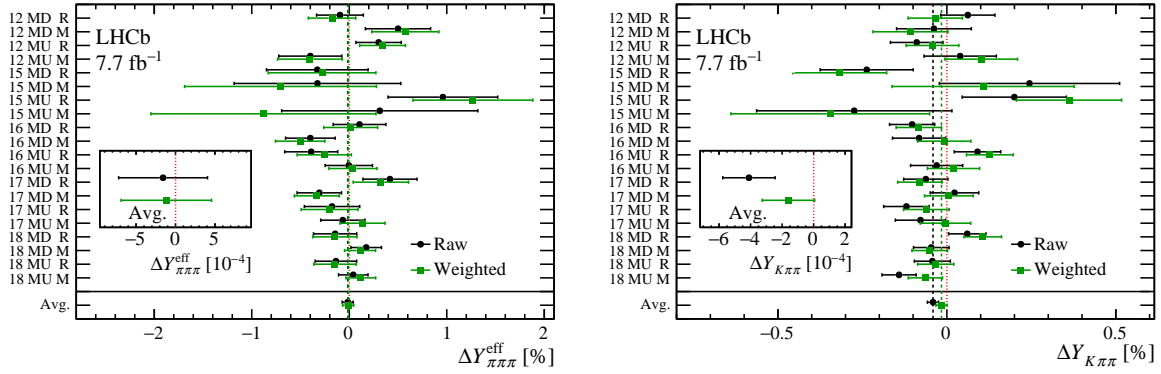


Figure 2: Measured gradient of the time-dependent asymmetry before and after kinematic weighting in each of the subsamples for (left) the signal channel and (right) the control channel. The abbreviation Avg. denotes the weighted average across all datasets obtained from a least squares fit, MU (MD) denotes the *MagUp* (*MagDown*) magnet polarity and M (R) denotes the merged (resolved)  $\pi^0$  category. The black and green dotted lines represent the average measured gradients before and after the kinematic weighting, respectively, and the red dotted line indicates a value of zero. Only statistical uncertainties are shown.

The measured value of  $\Delta Y_{K\pi\pi}$  is compatible with zero at the level of  $2.5\sigma$  before the kinematic weighting and  $1.0\sigma$  after the kinematic weighting, where  $\sigma$  is the statistical uncertainty. Finally, a set of pseudoexperiments is performed to evaluate and correct for the dilution of the measured  $\Delta Y$  caused by the kinematic weighting, since a true time-dependent asymmetry would induce some kinematic-dependent asymmetries through the aforementioned correlations.

The systematic uncertainties associated with the measured time-dependent asymmetries are given in Table 1 for both the signal and control modes. The dominant systematic uncertainties arise from possible kinematic-dependent detection asymmetries affecting the charged products of the  $D^0$  meson decay. Potential biases from such sources are assessed by measuring the raw asymmetry as a function of phase-space position and decay time using the decays  $D_{(s)}^+ \rightarrow \pi^+\pi^+\pi^-$ ,  $D_{(s)}^+ \rightarrow \phi(\rightarrow K^-K^+)\pi^+$ , and  $D^+ \rightarrow K^-\pi^+\pi^+$  as [11,24]

$$\begin{aligned}
 A_{\text{det}}^{\pi\pi} &= A_{D_{(s)}^+ \rightarrow \pi^+\pi^+\pi^-} - A_{D_{(s)}^+ \rightarrow \phi(\rightarrow K^-K^+)\pi^+}, \\
 A_{\text{det}}^{K\pi} &= A_{D^+ \rightarrow K^-\pi^+\pi^+} - A_{D^+ \rightarrow \phi(\rightarrow K^-K^+)\pi^+},
 \end{aligned}
 \tag{5}$$

where  $A_{\text{det}}^{\pi\pi}$  ( $A_{\text{det}}^{K\pi}$ ) represents the detection asymmetry between a  $\pi^+\pi^-$  ( $K^-\pi^+$ ) pair and its charge-conjugate at a given phase-space position and decay time. In each of these calibration decays, candidates are weighted so that the kinematic distributions agree between each pair of  $D_{(s)}^+$  decays. This ensures a precise cancellation of kinematic-dependent detection and production asymmetries affecting the  $D_{(s)}^+$  meson and the additional charged pion. Candidates are further weighted to align the kinematic distributions with those observed in the relevant  $D^0$  decay mode, to accurately reproduce any kinematic-dependent  $\pi^+\pi^-$  or  $K^-\pi^+$  detection asymmetries [24]. Potential direct  $CP$  asymmetries in the calibration modes do not induce kinematic or decay-time dependent effects and are therefore irrelevant in this procedure. The measured asymmetry maps are then used as inputs for a set of pseudoexperiments to determine the potential biases on  $\Delta Y_{\pi\pi\pi}^{\text{eff}}$  and  $\Delta Y_{K\pi\pi}$ .

Table 1: Systematic uncertainties affecting  $\Delta Y_{\pi\pi\pi}^{\text{eff}}$  ( $\Delta Y_{K\pi\pi}$ ) in the signal (control) channel.

Source	$\Delta Y_{\pi\pi\pi}^{\text{eff}}$ ( $10^{-4}$ )	$\Delta Y_{K\pi\pi}$ ( $10^{-4}$ )
Detection asymmetries	1.6	3.4
$t/\tau_{D^0}$ binning	1.0	0.14
Secondary contamination	0.84	0.84
$\Delta m$ fit model	0.75	0.08
Kinematic weighting	0.22	0.22
Total	2.3	3.5

A systematic uncertainty on the effect of the decay-time binning is conservatively assessed by performing the analysis with different choices of the decay-time binning scheme. The fraction of contamination from secondary decays and their asymmetries are measured in each decay-time bin by fitting the distribution of  $\ln \chi_{\text{IP}}^2$  for selected candidates using templates from simulation and the  $\Delta m$  sideband data as input. The measured fractions and asymmetries are then used in a pseudoexperiment study to determine the resulting systematic uncertainty. An average secondary fraction at the percent level is observed, depending on the data-taking period and  $\pi^0$  candidate reconstruction category. The uncertainty arising from the  $\Delta m$  fit model is assessed in a set of pseudoexperiments using an alternative fit model to describe the signal and background  $\Delta m$  distributions. The number of bins used in the kinematic weighting is varied between a factor of one half and two, and the resulting standard deviation of measured asymmetry gradients is taken as a systematic uncertainty. A set of pseudoexperiments is carried out to determine the dilution of the measured asymmetry due to the finite decay-time resolution. The differences between the measured gradients with and without correcting for this effect are found to be negligible. Finally, the uncertainty on the measured  $\Delta Y_{\pi\pi\pi}^{\text{eff}}$  related to the externally measured  $D^0$  lifetime [14, 15] is found to be negligible. No statistically significant effects are observed when stability checks are performed by applying a hardware-trigger requirement or adopting different strategies for the kinematic weighting and yield determination. Systematic uncertainties associated with the knowledge of the externally measured  $CP$ -even fraction and the effect of a nonuniform phase-space acceptance on its central value are found to be negligible.

By performing a least-squares fit to the measured asymmetry gradients in all subsets of the data, the final result  $\Delta Y_{\pi\pi\pi}^{\text{eff}} = (-1.2 \pm 6.0 \pm 2.3) \times 10^{-4}$  is obtained. The first uncertainty is statistical and the second is systematic, here and in the following. No evidence for time-dependent  $CP$  violation in this channel is found. This corresponds, using the externally measured  $CP$ -even fraction [26], to

$$\Delta Y = (-1.3 \pm 6.3 \pm 2.4) \times 10^{-4}.$$

This result is in excellent agreement with the current world average [12]. In the control channel, the measurement  $\Delta Y_{K\pi\pi} = (-1.7 \pm 1.8 \pm 3.5) \times 10^{-4}$  is obtained, which validates the kinematic-weighting procedure designed to account for nuisance asymmetries. Figure 3 shows the measured asymmetry for all selected  $D^0 \rightarrow \pi^+\pi^-\pi^0$  and  $D^0 \rightarrow K^-\pi^+\pi^0$  candidates as a function of decay time, along with a linear fit.

In summary, a measurement of time-dependent  $CP$  violation in the decay  $D^0 \rightarrow \pi^+\pi^-\pi^0$



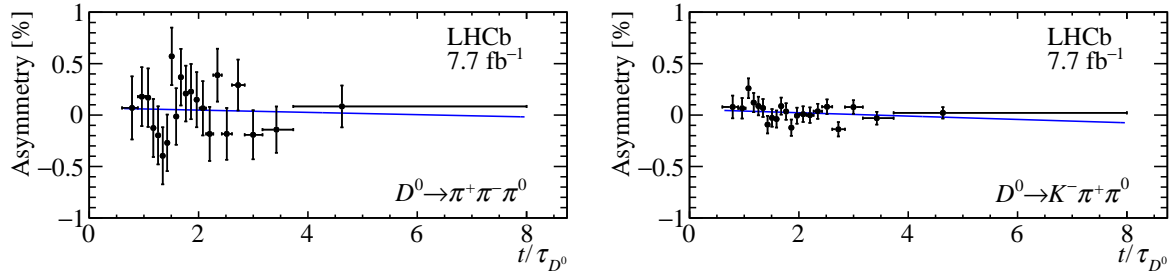


Figure 3: Measured asymmetry of (left)  $D^0 \rightarrow \pi^+ \pi^- \pi^0$  and (right)  $D^0 \rightarrow K^- \pi^+ \pi^0$  decays as a function of decay time, after kinematic weighting. The  $\chi^2$  per degree of freedom of the linear fits shown alongside the data are 17/19 and 22/19, respectively.

has been presented. No evidence for  $CP$  violation is found. The precision of this measurement is limited by the statistical uncertainty and the result is in excellent agreement with the current world average of the parameter  $\Delta Y$ . This represents the first measurement of time-dependent  $CP$  violation in the singly Cabibbo-suppressed decay  $D^0 \rightarrow \pi^+ \pi^- \pi^0$ .

## Acknowledgements

We express our gratitude to our colleagues in the CERN accelerator departments for the excellent performance of the LHC. We thank the technical and administrative staff at the LHCb institutes. We acknowledge support from CERN and from the national agencies: CAPES, CNPq, FAPERJ and FINEP (Brazil); MOST and NSFC (China); CNRS/IN2P3 (France); BMBF, DFG and MPG (Germany); INFN (Italy); NWO (Netherlands); MNiSW and NCN (Poland); MCID/IFA (Romania); MICINN (Spain); SNSF and SER (Switzerland); NASU (Ukraine); STFC (United Kingdom); DOE NP and NSF (USA). We acknowledge the computing resources that are provided by CERN, IN2P3 (France), KIT and DESY (Germany), INFN (Italy), SURF (Netherlands), PIC (Spain), GridPP (United Kingdom), CSCS (Switzerland), IFIN-HH (Romania), CBPF (Brazil), and Polish WLCG (Poland). We are indebted to the communities behind the multiple open-source software packages on which we depend. Individual groups or members have received support from ARC and ARDC (Australia); Key Research Program of Frontier Sciences of CAS, CAS PIFI, CAS CCEPP, Fundamental Research Funds for the Central Universities, and Sci. & Tech. Program of Guangzhou (China); Minciencias (Colombia); EPLANET, Marie Skłodowska-Curie Actions, ERC and NextGenerationEU (European Union); A\*MIDEX, ANR, IPhU and Labex P2IO, and Région Auvergne-Rhône-Alpes (France); AvH Foundation (Germany); ICSC (Italy); GVA, XuntaGal, GENCAT, Inditex, InTalent and Prog. Atracción Talento, CM (Spain); SRC (Sweden); the Leverhulme Trust, the Royal Society and UKRI (United Kingdom).

## References

- [1] A. D. Sakharov, *Violation of CP invariance, C asymmetry, and baryon asymmetry of the universe*, Pisma Zh. Eksp. Teor. Fiz. **5** (1967) 32.

- [2] M. Dine and A. Kusenko, *Origin of the matter - antimatter asymmetry*, Rev. Mod. Phys. **76** (2003) 1, arXiv:hep-ph/0303065.
- [3] L. Canetti, M. Drewes, and M. Shaposhnikov, *Matter and antimatter in the universe*, New J. Phys. **14** (2012) 095012, arXiv:1204.4186.
- [4] J. H. Christenson, J. W. Cronin, V. L. Fitch, and R. Turlay, *Evidence for the  $2\pi$  decay of the  $K_2^0$  meson*, Phys. Rev. Lett. **13** (1964) 138.
- [5] KTeV collaboration, A. Alavi-Harati *et al.*, *Observation of direct CP violation in  $K_{S,L} \rightarrow \pi\pi$  decays*, Phys. Rev. Lett. **83** (1999) 22, arXiv:hep-ex/9905060.
- [6] BaBar collaboration, B. Aubert *et al.*, *Observation of CP violation in the  $B^0$  meson system*, Phys. Rev. Lett. **87** (2001) 091801, arXiv:hep-ex/0107013.
- [7] Belle collaboration, K. Abe *et al.*, *Observation of large CP violation in the neutral B meson system*, Phys. Rev. Lett. **87** (2001) 091802, arXiv:hep-ex/0107061.
- [8] LHCb collaboration, R. Aaij *et al.*, *First observation of CP violation in the decays of  $B_s^0$  mesons*, Phys. Rev. Lett. **110** (2013) 221601, arXiv:1304.6173.
- [9] LHCb collaboration, R. Aaij *et al.*, *Observation of CP violation in two-body  $B_{(s)}^0$ -meson decays to charged pions and kaons*, JHEP **03** (2021) 075, arXiv:2012.05319.
- [10] LHCb collaboration, R. Aaij *et al.*, *Observation of CP violation in charm decays*, Phys. Rev. Lett. **122** (2019) 211803, arXiv:1903.08726.
- [11] LHCb collaboration, R. Aaij *et al.*, *Measurement of the time-integrated CP asymmetry in  $D^0 \rightarrow K^- K^+$  decays*, Phys. Rev. Lett. **131** (2023) 091802, arXiv:2209.03179.
- [12] Y. Amhis *et al.*, *Averages of b-hadron, c-hadron, and  $\tau$ -lepton properties as of 2021*, Phys. Rev. **D107** (2023) 052008, arXiv:2206.07501, updated results and plots available at <https://hflav.web.cern.ch>.
- [13] LHCb collaboration, *Simultaneous determination of the CKM angle  $\gamma$  and parameters related to mixing and CP violation in the charm sector*, LHCb-CONF-2022-003, 2022.
- [14] Particle Data Group, R. L. Workman *et al.*, *Review of particle physics*, Prog. Theor. Exp. Phys. **2022** (2022) 083C01.
- [15] Belle-II collaboration, F. Abudinén *et al.*, *Precise measurement of the  $D^0$  and  $D^+$  lifetimes at Belle II*, Phys. Rev. Lett. **127** (2021) 211801, arXiv:2108.03216.
- [16] A. L. Kagan and L. Silvestrini, *Dispersive and absorptive CP violation in  $D^0 - \bar{D}^0$  mixing*, Phys. Rev. **D103** (2021) 053008, arXiv:2001.07207.
- [17] BaBar collaboration, J. P. Lees *et al.*, *Measurement of  $D^0 - \bar{D}^0$  mixing and CP violation in two-body  $D^0$  Decays*, Phys. Rev. **D87** (2013) 012004, arXiv:1209.3896.

- [18] CDF collaboration, T. A. Aaltonen *et al.*, *Measurement of indirect CP-violating asymmetries in  $D^0 \rightarrow K^+K^-$  and  $D^0 \rightarrow \pi^+\pi^-$  decays at CDF*, Phys. Rev. **D90** (2014) 111103, [arXiv:1410.5435](#).
- [19] Belle collaboration, M. Starič *et al.*, *Measurement of  $D^0 - \bar{D}^0$  mixing and search for CP violation in  $D^0 \rightarrow K^+K^-$ ,  $\pi^+\pi^-$  decays with the full Belle data set*, Phys. Lett. **B753** (2016) 412, [arXiv:1509.08266](#).
- [20] LHCb collaboration, R. Aaij *et al.*, *Measurement of indirect CP asymmetries in  $D^0 \rightarrow K^-K^+$  and  $D^0 \rightarrow \pi^-\pi^+$  decays using semileptonic B decays*, JHEP **04** (2015) 043, [arXiv:1501.06777](#).
- [21] LHCb collaboration, R. Aaij *et al.*, *Measurement of the CP violation parameter  $A_\Gamma$  in  $D^0 \rightarrow K^+K^-$  and  $D^0 \rightarrow \pi^+\pi^-$  decays*, Phys. Rev. Lett. **118** (2017) 261803, [arXiv:1702.06490](#).
- [22] LHCb collaboration, R. Aaij *et al.*, *Updated measurement of decay-time-dependent CP asymmetries in  $D^0 \rightarrow K^+K^-$  and  $D^0 \rightarrow \pi^+\pi^-$  decays*, Phys. Rev. **D101** (2020) 012005, [arXiv:1911.01114](#).
- [23] LHCb collaboration, R. Aaij *et al.*, *Search for time-dependent CP violation in  $D^0 \rightarrow K^+K^-$  and  $D^0 \rightarrow \pi^+\pi^-$  decays*, Phys. Rev. **D104** (2021) 072010, [arXiv:2105.09889](#).
- [24] LHCb collaboration, R. Aaij *et al.*, *Observation of the mass difference between neutral charm-meson eigenstates*, Phys. Rev. Lett. **127** (2021) 111801, Erratum *ibid.* **131** (2023) 079901, [arXiv:2106.03744](#).
- [25] LHCb collaboration, R. Aaij *et al.*, *Model-independent measurement of charm mixing parameters in  $\bar{B} \rightarrow D^0(\rightarrow K^{*0}\pi^+\pi^-)\mu^-\bar{\nu}_\mu X$  decays*, Phys. Rev. **D108** (2023) 052005, [arXiv:2208.06512](#).
- [26] S. Malde *et al.*, *First determination of the CP content of  $D \rightarrow \pi^+\pi^-\pi^+\pi^-$  and updated determination of the CP contents of  $D \rightarrow \pi^+\pi^-\pi^0$  and  $D \rightarrow K^+K^-\pi^0$* , Phys. Lett. **B747** (2015) 9, [arXiv:1504.05878](#).
- [27] S. Malde, C. Thomas, and G. Wilkinson, *Measuring CP violation and mixing in charm with inclusive self-conjugate multibody decay modes*, Phys. Rev. **D91** (2015) 094032, [arXiv:1502.04560](#).
- [28] LHCb collaboration, A. A. Alves Jr. *et al.*, *The LHCb detector at the LHC*, JINST **3** (2008) S08005.
- [29] LHCb collaboration, R. Aaij *et al.*, *LHCb detector performance*, Int. J. Mod. Phys. **A30** (2015) 1530022, [arXiv:1412.6352](#).
- [30] LHCb collaboration, R. Aaij *et al.*, *Search for CP violation in  $D^0 \rightarrow \pi^-\pi^+\pi^0$  decays with the energy test*, Phys. Lett. **B740** (2015) 158, [arXiv:1410.4170](#).
- [31] V. V. Gligorov and M. Williams, *Efficient, reliable and fast high-level triggering using a bonsai boosted decision tree*, JINST **8** (2013) P02013, [arXiv:1210.6861](#).

- [32] W. D. Hulsbergen, *Decay chain fitting with a Kalman filter*, Nucl. Instrum. Meth. **A552** (2005) 566, [arXiv:physics/0503191](#).
- [33] R. Brun and F. Rademakers, *ROOT: An object oriented data analysis framework*, Nucl. Instrum. Meth. **A389** (1997) 81.
- [34] W. Verkerke and D. P. Kirkby, *The RooFit toolkit for data modeling*, eConf **C0303241** (2003) MOLT007, [arXiv:physics/0306116](#).



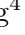





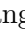



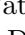












C. Wang<sup>20</sup> , G. Wang<sup>8</sup> , J. Wang<sup>6</sup> , J. Wang<sup>5</sup> , J. Wang<sup>4</sup> , J. Wang<sup>72</sup> , M. Wang<sup>28</sup> ,  
N. W. Wang<sup>7</sup> , R. Wang<sup>53</sup> , X. Wang<sup>8</sup> , X. Wang<sup>70</sup> , X. W. Wang<sup>60</sup> , Z. Wang<sup>13</sup> ,  
Z. Wang<sup>4</sup> , Z. Wang<sup>28</sup> , J.A. Ward<sup>55,1</sup> , M. Waterlaet<sup>47</sup> , N.K. Watson<sup>52</sup> ,  
D. Websdale<sup>60</sup> , Y. Wei<sup>6</sup> , J. Wendel<sup>78</sup> , B.D.C. Westhenry<sup>53</sup> , D.J. White<sup>61</sup> ,  
M. Whitehead<sup>58</sup> , A.R. Wiederhold<sup>55</sup> , D. Wiedner<sup>18</sup> , G. Wilkinson<sup>62</sup> ,  
M.K. Wilkinson<sup>64</sup> , M. Williams<sup>63</sup> , M.R.J. Williams<sup>57</sup> , R. Williams<sup>54</sup> , F.F. Wilson<sup>56</sup> ,  
W. Wislicki<sup>40</sup> , M. Witek<sup>39</sup> , L. Witola<sup>20</sup> , C.P. Wong<sup>66</sup> , G. Wormser<sup>13</sup> ,  
S.A. Wotton<sup>54</sup> , H. Wu<sup>67</sup> , J. Wu<sup>8</sup> , Y. Wu<sup>6</sup> , K. Wyllie<sup>47</sup> , S. Xian<sup>70</sup> , Z. Xiang<sup>5</sup> ,  
Y. Xie<sup>8</sup> , A. Xu<sup>33</sup> , J. Xu<sup>7</sup> , L. Xu<sup>4</sup> , L. Xu<sup>4</sup> , M. Xu<sup>55</sup> , Z. Xu<sup>11</sup> , Z. Xu<sup>7</sup> ,  
Z. Xu<sup>5</sup> , D. Yang<sup>4</sup> , S. Yang<sup>7</sup> , X. Yang<sup>6</sup> , Y. Yang<sup>27,n</sup> , Z. Yang<sup>6</sup> , Z. Yang<sup>65</sup> ,  
V. Yeroshenko<sup>13</sup> , H. Yeung<sup>61</sup> , H. Yin<sup>8</sup> , C. Y. Yu<sup>6</sup> , J. Yu<sup>69</sup> , X. Yuan<sup>5</sup> ,  
E. Zaffaroni<sup>48</sup> , M. Zavertyaev<sup>19</sup> , M. Zdybal<sup>39</sup> , C. Zeng<sup>5,7</sup> , M. Zeng<sup>4</sup> , C. Zhang<sup>6</sup> ,  
D. Zhang<sup>8</sup> , J. Zhang<sup>7</sup> , L. Zhang<sup>4</sup> , S. Zhang<sup>69</sup> , S. Zhang<sup>6</sup> , Y. Zhang<sup>6</sup> , Y. Z.  
Zhang<sup>4</sup> , Y. Zhao<sup>20</sup> , A. Zharkova<sup>42</sup> , A. Zhelezov<sup>20</sup> , X. Z. Zheng<sup>4</sup> , Y. Zheng<sup>7</sup> ,  
T. Zhou<sup>6</sup> , X. Zhou<sup>8</sup> , Y. Zhou<sup>7</sup> , V. Zhovkovska<sup>55</sup> , L. Z. Zhu<sup>7</sup> , X. Zhu<sup>4</sup> ,  
X. Zhu<sup>8</sup> , V. Zhukov<sup>16</sup> , J. Zhuo<sup>46</sup> , Q. Zou<sup>5,7</sup> , D. Zuliani<sup>31,q</sup> , G. Zunica<sup>48</sup> .

<sup>1</sup>*School of Physics and Astronomy, Monash University, Melbourne, Australia*

<sup>2</sup>*Centro Brasileiro de Pesquisas Físicas (CBPF), Rio de Janeiro, Brazil*

<sup>3</sup>*Universidade Federal do Rio de Janeiro (UFRJ), Rio de Janeiro, Brazil*

<sup>4</sup>*Center for High Energy Physics, Tsinghua University, Beijing, China*

<sup>5</sup>*Institute Of High Energy Physics (IHEP), Beijing, China*

<sup>6</sup>*School of Physics State Key Laboratory of Nuclear Physics and Technology, Peking University, Beijing, China*

<sup>7</sup>*University of Chinese Academy of Sciences, Beijing, China*

<sup>8</sup>*Institute of Particle Physics, Central China Normal University, Wuhan, Hubei, China*

<sup>9</sup>*Consejo Nacional de Rectores (CONARE), San Jose, Costa Rica*

<sup>10</sup>*Université Savoie Mont Blanc, CNRS, IN2P3-LAPP, Annecy, France*

<sup>11</sup>*Université Clermont Auvergne, CNRS/IN2P3, LPC, Clermont-Ferrand, France*

<sup>12</sup>*Aix Marseille Univ, CNRS/IN2P3, CPPM, Marseille, France*

<sup>13</sup>*Université Paris-Saclay, CNRS/IN2P3, IJCLab, Orsay, France*

<sup>14</sup>*Laboratoire Leprince-Ringuet, CNRS/IN2P3, Ecole Polytechnique, Institut Polytechnique de Paris, Palaiseau, France*

<sup>15</sup>*LPNHE, Sorbonne Université, Paris Diderot Sorbonne Paris Cité, CNRS/IN2P3, Paris, France*

<sup>16</sup>*I. Physikalisches Institut, RWTH Aachen University, Aachen, Germany*

<sup>17</sup>*Universität Bonn - Helmholtz-Institut für Strahlen und Kernphysik, Bonn, Germany*

<sup>18</sup>*Fakultät Physik, Technische Universität Dortmund, Dortmund, Germany*

<sup>19</sup>*Max-Planck-Institut für Kernphysik (MPIK), Heidelberg, Germany*

<sup>20</sup>*Physikalisches Institut, Ruprecht-Karls-Universität Heidelberg, Heidelberg, Germany*

<sup>21</sup>*School of Physics, University College Dublin, Dublin, Ireland*

<sup>22</sup>*INFN Sezione di Bari, Bari, Italy*

<sup>23</sup>*INFN Sezione di Bologna, Bologna, Italy*

<sup>24</sup>*INFN Sezione di Ferrara, Ferrara, Italy*

<sup>25</sup>*INFN Sezione di Firenze, Firenze, Italy*

<sup>26</sup>*INFN Laboratori Nazionali di Frascati, Frascati, Italy*

<sup>27</sup>*INFN Sezione di Genova, Genova, Italy*

<sup>28</sup>*INFN Sezione di Milano, Milano, Italy*

<sup>29</sup>*INFN Sezione di Milano-Bicocca, Milano, Italy*

<sup>30</sup>*INFN Sezione di Cagliari, Monserrato, Italy*

<sup>31</sup>*INFN Sezione di Padova, Padova, Italy*

<sup>32</sup>*INFN Sezione di Perugia, Perugia, Italy*

<sup>33</sup>*INFN Sezione di Pisa, Pisa, Italy*

<sup>34</sup>*INFN Sezione di Roma La Sapienza, Roma, Italy*

<sup>35</sup>*INFN Sezione di Roma Tor Vergata, Roma, Italy*

<sup>36</sup>*Nikhef National Institute for Subatomic Physics, Amsterdam, Netherlands*

- <sup>37</sup> *Nikhef National Institute for Subatomic Physics and VU University Amsterdam, Amsterdam, Netherlands*
- <sup>38</sup> *AGH - University of Krakow, Faculty of Physics and Applied Computer Science, Kraków, Poland*
- <sup>39</sup> *Henryk Niewodniczanski Institute of Nuclear Physics Polish Academy of Sciences, Kraków, Poland*
- <sup>40</sup> *National Center for Nuclear Research (NCBJ), Warsaw, Poland*
- <sup>41</sup> *Horia Hulubei National Institute of Physics and Nuclear Engineering, Bucharest-Magurele, Romania*
- <sup>42</sup> *Affiliated with an institute covered by a cooperation agreement with CERN*
- <sup>43</sup> *DS4DS, La Salle, Universitat Ramon Llull, Barcelona, Spain*
- <sup>44</sup> *ICCUB, Universitat de Barcelona, Barcelona, Spain*
- <sup>45</sup> *Instituto Galego de Física de Altas Enerxías (IGFAE), Universidade de Santiago de Compostela, Santiago de Compostela, Spain*
- <sup>46</sup> *Instituto de Física Corpuscular, Centro Mixto Universidad de Valencia - CSIC, Valencia, Spain*
- <sup>47</sup> *European Organization for Nuclear Research (CERN), Geneva, Switzerland*
- <sup>48</sup> *Institute of Physics, Ecole Polytechnique Fédérale de Lausanne (EPFL), Lausanne, Switzerland*
- <sup>49</sup> *Physik-Institut, Universität Zürich, Zürich, Switzerland*
- <sup>50</sup> *NSC Kharkiv Institute of Physics and Technology (NSC KIPT), Kharkiv, Ukraine*
- <sup>51</sup> *Institute for Nuclear Research of the National Academy of Sciences (KINR), Kyiv, Ukraine*
- <sup>52</sup> *University of Birmingham, Birmingham, United Kingdom*
- <sup>53</sup> *H.H. Wills Physics Laboratory, University of Bristol, Bristol, United Kingdom*
- <sup>54</sup> *Cavendish Laboratory, University of Cambridge, Cambridge, United Kingdom*
- <sup>55</sup> *Department of Physics, University of Warwick, Coventry, United Kingdom*
- <sup>56</sup> *STFC Rutherford Appleton Laboratory, Didcot, United Kingdom*
- <sup>57</sup> *School of Physics and Astronomy, University of Edinburgh, Edinburgh, United Kingdom*
- <sup>58</sup> *School of Physics and Astronomy, University of Glasgow, Glasgow, United Kingdom*
- <sup>59</sup> *Oliver Lodge Laboratory, University of Liverpool, Liverpool, United Kingdom*
- <sup>60</sup> *Imperial College London, London, United Kingdom*
- <sup>61</sup> *Department of Physics and Astronomy, University of Manchester, Manchester, United Kingdom*
- <sup>62</sup> *Department of Physics, University of Oxford, Oxford, United Kingdom*
- <sup>63</sup> *Massachusetts Institute of Technology, Cambridge, MA, United States*
- <sup>64</sup> *University of Cincinnati, Cincinnati, OH, United States*
- <sup>65</sup> *University of Maryland, College Park, MD, United States*
- <sup>66</sup> *Los Alamos National Laboratory (LANL), Los Alamos, NM, United States*
- <sup>67</sup> *Syracuse University, Syracuse, NY, United States*
- <sup>68</sup> *Pontifícia Universidade Católica do Rio de Janeiro (PUC-Rio), Rio de Janeiro, Brazil, associated to <sup>3</sup>*
- <sup>69</sup> *School of Physics and Electronics, Hunan University, Changsha City, China, associated to <sup>8</sup>*
- <sup>70</sup> *Guangdong Provincial Key Laboratory of Nuclear Science, Guangdong-Hong Kong Joint Laboratory of Quantum Matter, Institute of Quantum Matter, South China Normal University, Guangzhou, China, associated to <sup>4</sup>*
- <sup>71</sup> *Lanzhou University, Lanzhou, China, associated to <sup>5</sup>*
- <sup>72</sup> *School of Physics and Technology, Wuhan University, Wuhan, China, associated to <sup>4</sup>*
- <sup>73</sup> *Departamento de Física, Universidad Nacional de Colombia, Bogota, Colombia, associated to <sup>15</sup>*
- <sup>74</sup> *Eotvos Lorand University, Budapest, Hungary, associated to <sup>47</sup>*
- <sup>75</sup> *Van Swinderen Institute, University of Groningen, Groningen, Netherlands, associated to <sup>36</sup>*
- <sup>76</sup> *Universiteit Maastricht, Maastricht, Netherlands, associated to <sup>36</sup>*
- <sup>77</sup> *Tadeusz Kosciuszko Cracow University of Technology, Cracow, Poland, associated to <sup>39</sup>*
- <sup>78</sup> *Universidade da Coruña, A Coruña, Spain, associated to <sup>43</sup>*
- <sup>79</sup> *Department of Physics and Astronomy, Uppsala University, Uppsala, Sweden, associated to <sup>58</sup>*
- <sup>80</sup> *University of Michigan, Ann Arbor, MI, United States, associated to <sup>67</sup>*
- <sup>81</sup> *Departement de Physique Nucleaire (SPhN), Gif-Sur-Yvette, France*

<sup>a</sup> *Universidade de Brasília, Brasília, Brazil*

<sup>b</sup> *Centro Federal de Educação Tecnológica Celso Suckow da Fonseca, Rio De Janeiro, Brazil*

<sup>c</sup> *Hangzhou Institute for Advanced Study, UCAS, Hangzhou, China*

<sup>d</sup> *School of Physics and Electronics, Henan University, Kaifeng, China*

<sup>e</sup> *LIP6, Sorbonne Universite, Paris, France*

<sup>f</sup> *Excellence Cluster ORIGINS, Munich, Germany*

<sup>g</sup> *Universidad Nacional Autónoma de Honduras, Tegucigalpa, Honduras*

- <sup>h</sup> *Università di Bari, Bari, Italy*  
<sup>i</sup> *Università degli studi di Bergamo, Bergamo, Italy*  
<sup>j</sup> *Università di Bologna, Bologna, Italy*  
<sup>k</sup> *Università di Cagliari, Cagliari, Italy*  
<sup>l</sup> *Università di Ferrara, Ferrara, Italy*  
<sup>m</sup> *Università di Firenze, Firenze, Italy*  
<sup>n</sup> *Università di Genova, Genova, Italy*  
<sup>o</sup> *Università degli Studi di Milano, Milano, Italy*  
<sup>p</sup> *Università degli Studi di Milano-Bicocca, Milano, Italy*  
<sup>q</sup> *Università di Padova, Padova, Italy*  
<sup>r</sup> *Università di Perugia, Perugia, Italy*  
<sup>s</sup> *Scuola Normale Superiore, Pisa, Italy*  
<sup>t</sup> *Università di Pisa, Pisa, Italy*  
<sup>u</sup> *Università della Basilicata, Potenza, Italy*  
<sup>v</sup> *Università di Roma Tor Vergata, Roma, Italy*  
<sup>w</sup> *Università di Siena, Siena, Italy*  
<sup>x</sup> *Università di Urbino, Urbino, Italy*  
<sup>y</sup> *Universidad de Alcalá, Alcalá de Henares, Spain*  
<sup>z</sup> *Facultad de Ciencias Físicas, Madrid, Spain*  
<sup>aa</sup> *Department of Physics/Division of Particle Physics, Lund, Sweden*  
<sup>†</sup> *Deceased*